Annals of Botany **123**: 1079–1088, 2019
doi: 10.1093/aob/mcz015, available online at www.academic.oup.com/aob

ANNALS OF BOTANY
Founded 1887

Phytochrome B enhances plant growth, biomass and grain yield in field-grown maize

Germán Wies[1,*], Anita Ida Mantese[2], Jorge José Casal[3,4] and Gustavo Ángel Maddonni[1,3]

[1]Cátedra de Cerealicultura, Facultad de Agronomía, UBA, Av. San Martín 4453, (C1417DSE), Ciudad Autónoma de Buenos Aires, Argentina, [2]Cátedra de Botánica General, Facultad de Agronomía, UBA, Av. San Martín 4453, (C1417DSE), Ciudad Autónoma de Buenos Aires, Argentina, [3]IFEVA, Facultad de Agronomía, Universidad de Buenos Aires and Consejo Nacional de Investigaciones Científicas y Técnicas, Av. San Martín 4453, (C1417DSE), Ciudad Autónoma de Buenos Aires, Argentina and [4]Fundación Instituto Leloir, Instituto de Investigaciones Bioquímicas de Buenos Aires–CONICET, 1405 Buenos Aires, Argentina
** For correspondence. Email gwies@agro.uba.ar*

Received: 10 April 2018 Returned for revision: 29 August 2018 Editorial decision: 10 January 2019 Accepted: 14 January 2019

• **Background and Aims** Phytochrome B (phyB) is a photosensory receptor important for the control of plant plasticity and resource partitioning. Whether phyB is required to optimize plant biomass accumulation in agricultural crops exposed to full sunlight is unknown. Here we investigated the impact of mutations in the genes that encode either phyB1 or phyB2 on plant growth and grain yield in field crops of *Zea mays* sown at contrasting population densities.
• **Methods** Plants of maize inbred line France 2 wild type (WT) and the isogenic mutants lacking either phyB1 or phyB2 (*phyB1* and *phyB2*) were cultivated in the field during two seasons. Plants were grown at two densities (9 and 30 plants m^{-2}), irrigated and without restrictions of nutrients. Leaf and stem growth, leaf anatomy, light interception, above-ground biomass accumulation and grain yield were recorded.
• **Key Results** At high plant density, all the lines showed similar kinetics of biomass accumulation. However, compared with the WT, the *phyB1* and *phyB2* mutations impaired the ability to enhance plant growth in response to the additional resources available at low plant density. This effect was largely due to a reduced leaf area (fewer cells per leaf), which compromised light interception capacity. Grain yield was reduced in *phyB1* plants.
• **Conclusions** Maize plants grown in the field at relatively low densities require phyB1 and phyB2 to sense the light environment and optimize the use of the available resources. In the absence of either of these two light receptors, leaf expansion is compromised, imposing a limitation to the interception of photosynthetic radiation and growth. These observations suggest that genetic variability at the locus encoding phyB could offer a breeding target to improve crop growth capacity in the field.

Key words: Maize, *Zea mays*, phytochrome B, red/far-red ratio, plant density, plant growth.

INTRODUCTION

Plants use light for photosynthesis, but also as a source of information about their surrounding environment (Casal, 2013*a*, *b*; Ballaré and Pierik, 2017). Photosensory receptors such as phytochromes (phy) and cryptochromes detect variations in the light environment, triggering responses that help plants adjust their growth and development patterns. Phytochromes have two forms: the inactive form, which absorbs maximally in red light (Pr) and the active form, which absorbs maximally in far-red light (Pfr). Upon light excitation, Pr relaxes to the Pfr form, and vice versa. Therefore, the proportion of Pfr depends on the red/far-red ratio (R:FR) experienced by plants within a canopy (Smith *et al.*, 1990).

Monocots possess three phy gene clades called *PHYA*, *PHYB* and *PHYC* (Mathews and Sharrock, 1997; Kulshreshtha *et al.*, 2005). In maize, these genes are duplicated, presenting *PHYA1*, *PHYB1* and *PHYC1* genes on chromosome 1, *PHYA2* and *PHYC2* on chromosome 5S, and *PHYB2* on chromosome 9L (Sheehan *et al.*, 2004). phyB1 and phyB2 have both overlapping and non-redundant functions in the control of growth and development of maize (Sheehan *et al.*, 2007).

As sunlight penetrates through the canopy, the radiation in the wavelengths of UV, blue and red decreases in relation to the wavelengths of the green and particularly far-red due to the selective absorbance and reflection by the photosynthetic pigments of green tissues (Casal, 2013*a*, *b*; Ballaré and Pierik, 2017). Therefore, the R:FR decreases and this neighbour cue is perceived mainly by phyB as a reduction in its level of Pfr. In turn, low Pfr levels release the shade-avoidance responses, i.e. the changes in growth patterns that tend to decrease the degree of current or future shade (Casal, 2013*a*, *b*; Ballaré and Pierik, 2017).

As population density increases, maize plants are exposed to low irradiance values and low R:FR (Tetio-Kagho and Gardner, 1988; Sattin *et al.*, 1994; Maddonni *et al.*, 2001; Borrás *et al.*, 2003). This cue promotes shade-avoidance responses, such as suppression of tiller production, elongation and thinning of stems and leaves, and spatial reorientation of leaves (Tetio-Kagho and Gardner, 1988; Maddonni *et al.*, 2001; Sangoi *et al.*, 2002). Similar responses can be obtained with maize plants

grown in the field, by using selective light filters that simulate the presence of neighbours (Maddonni *et al.*, 2002) or non-shading green leaves that reflect far-red light without shading the maize plants (Page *et al.*, 2009, 2011). The observation that maize plants deficient in phyB1 and/or phyB2 show morphological features of shade avoidance in the absence of neighbour signals further supports the role of these photosensory receptors in the adjustment of the plant body form to the presence of neighbours (Sheehan *et al.*, 2007).

In addition to a constitutive shade-avoidance phenotype, mutants of multiple photosensory receptors can show reductions in their overall growth capacity. For instance, in *Arabidopsis thaliana*, mutations in *phyB phyD* and *phyA phyB phyD phyE* reduce growth, biomass accumulation, chlorophyll contents, CO_2 uptake and the release of sucrose and starch during the day (Yang *et al.*, 2016). Similarly, mutations in *phyA phyB cry1 cry2* reduce growth and the rate of leaf appearance (Mazzella *et al.*, 2001). The quintuple *phyA phyB phyC phyD phyE* lacking all phys, shows severely impaired growth (Strasser *et al.*, 2010). Therefore, in addition to repressing shade-avoidance responses, photosensory receptors have a role in the control of the basic growth capacity (Yang *et al.*, 2016). Whether this control is a feature exclusive to *A. thaliana* plants grown under the relatively low light of controlled conditions remains to be elucidated.

The aim of this work is to investigate if the *phyB1* and/or *phyB2* mutations affect the growth capacity and selected morphological traits of maize plants in the field. This analysis was conducted at two contrasting plant densities because this allowed us to evaluate the interactions between phyB deficiency and the changes in light conditions.

MATERIALS AND METHODS

Plant material

Plants of maize (*Zea mays*) with mutations in the genes that encode either phyB1 (*phyB1*) or phyB2 (*phyB2*) were compared with their near-isogenic siblings of the France 2 background used as wild type (WT) (Sheehan *et al.*, 2007). The *phyB1-563* allele bears a *Mu* transposon insertion located upstream of a conserved cysteine residue in the GAF domain of phy, and the original line was back-crossed to France 2 four times (Sheehan *et al.*, 2007). The *phyB2-F2* mutant is a natural loss-of-function allele of the France 2 inbred line (Sheehan *et al.*, 2007). Therefore, a WT *PHY2* allele from the *Mutator* parent of unknown ancestry was introduced to obtain the single *phyB1* mutant and the line used as the WT (Sheehan *et al.*, 2007). Seeds of these genotypes were provided by the Maize Genetics Cooperation Stock Center (http://maizecoop.cropsci.uiuc.edu).

Population density experiments

Two field experiments were conducted to investigate the growth patterns of the WT and the *phyB1* and *phyB2* mutants at two contrasting population densities. The experiments were carried out on a silty clay loam soil (Vertic Argiudoll, Soil Taxonomy, U.S. Department of Agriculture) at the experimental unit of the Department of Plant Production of the University of Buenos Aires, Argentina (34°25'S, 58°25'W). Sowing dates were 15 January 2009 (Exp_1) and 18 November 2011 (Exp_2). Mean air temperature was similar during Exp_1 (23.6 °C) and Exp_2 (23.8 °C). Accumulated incident solar radiation during Exp_2 (2473.3 MJ m^{-2}) was significantly higher than that during Exp_1 (1486.8 MJ m^{-2}).

Treatments of Exp_1 and Exp_2 were arranged in a split-plot design with three replicates, with plant population density as the main factor (9 and 30 plants m^{-2}), and the genotype as the sub-factor (i.e. sub-plot). Each sub-plot involved three rows, 3 m long and 0.40 m apart. Rows had an east–west orientation. Although the two densities could be considered high for maize hybrids plants, which produce more biomass, for the small plant size of the lines used here a density of 9 plants m^{-2} is deemed low.

To ensure an even seedling distribution along the row and to avoid premature leaf interference (Toler *et al.*, 1999), two seeds per position were fixed on adhesive paper tapes at the corresponding interval of each plant density (8 and 27 cm, for the high and the low plant density). The tip cap was placed pointing down and the embryo face parallel to the row. Consequently, the first leaf of seedlings grew northwards, and the successive leaves grew mostly perpendicular to the rows. After seedling emergence, sub-plots were hand-thinned, leaving one plant per position, and ten aligned plants of the central row of each sub-plot were tagged for measurements. Crops were drip-irrigated during the cycle, and N fertilization (200 kg N ha^{-1}) was applied at the four ligulated-leaf stage (V_4; Ritchie *et al.*, 1993) to minimize N restrictions. Weeds, diseases and insects were chemically controlled.

Plant growth and grain yield

Above-ground plant biomass (hereafter plant biomass) was estimated by means of allometric models broadly used in this species (Maddonni and Otegui, 2004; Echarte and Tollenaar, 2006; Pagano and Maddonni, 2007; Laserna *et al.*, 2012). Weekly during the cycle, equal morphometric measurements were recorded from both tagged and harvested plants growing at similar conditions in Exp_1 and Exp_2. From V_3 to 15 d after female flowering (R_3; Ritchie *et al.*, 1993), plant height from ground level to the ligule of the uppermost leaf and basal stem diameter were recorded weekly in tagged plants. These data allowed us to calculate shoot volume by using a cylinder equation. In parallel, each measuring day, other plants of each genotype (WT, *phyB1* and *phyB2*) were harvested and equally measured to obtain shoot volume. Linear models were fitted between plant biomass (on a dry weight basis) and shoot volume from harvested plants. These models were used to estimate plant biomass of tagged plants durng the cycle (Supplementary Data Table S1).

To estimate ear biomass at female flowering (R_1) and R_3, exponential models were fitted between the maximum ear diameter and ear dry weight (husks + cob + florets) from sampled ears of each genotype. Maximum ear diameter data were also recorded in tagged plants to estimate ear biomass. Model parameters are listed in Supplementary Data Table S1.

The growth rate of tagged plants (PGR) around R_1 (i.e. the critical period) was calculated as the slope of the regression fitted to individual plant biomass at V_{10}, R_1 and R_3, and time after sowing.

At physiological maturity (R_6), tagged plants were individually harvested and weighed after 72 h of drying in a stove. Plant grain yield was estimated from the dry weight of kernels of each tagged plant. Plant fertility index was calculated as the ratio between the number of fertile ears (i.e. ears with >10 kernels; Tollenaar *et al.*, 1992) and the number of sampled plants per plot.

Plant leaf area and stem dimensions

The number of ligulated leaves, leaf dimensions (length and width), plant height (from ground level to the insertion of the uppermost expanded leaf) and basal stem diameter were recorded weekly on tagged plants of Exp_1 and Exp_2. Leaf size (S) was estimated based on the length (L) and maximum width (W) of each fully expanded leaf as described by Montgomery (1911) in eqn (1):

$$S = \alpha LW \quad (1)$$

where $\alpha = 0.75$ for a wide range of genotypes and densities (Stewart and Dwyer, 1999).

Total leaf area per plant (PLA) was calculated as the sum of the S of green leaves at R_1. A leaf was considered senesced when at least half of its area had yellowed.

Leaf anatomy

To describe leaf anatomy, the leaf inserted immediately below the apical ear (ear leaf) was sampled from three plants of each sub-plot only in Exp_2. The ear leaf is among the largest leaves of maize plants and its size differs among genotypes and plant densities (Tollenaar *et al.*, 1992; Maddonni and Otegui, 1996; Maddonni *et al.*, 2001). Three portions from the central part of each lamina were cut and dissected to analyse cell layers of both adaxail and abaxial surfaces. Both layers were diaphanized by using the technique of Dizeo de Strittmater (1973) and stained with safranin-fast green (Johansen, 1940). Sections were photographed with a Zeiss Axioplan optical microscope (Oberkochen, Germany) and analysed with the Zeiss AxioCam ERc 5s software (Jena, Germany). Total cell number, cell width, cell length and number of stomata were measured in a standardized area (30 000 μm^2). Transversal cuts were done to determine leaf width. Thin slices (approx. 10–15 µm thick) were cut with a Mino-type rotary microtome and embedded in paraffin. These samples were stained in the same way as described above.

Azimuthal distribution of leaves

In Exp_1 and Exp_2, the azimuthal distribution of leaves was measured after the leaf expansion period (i.e. immediately after R_1) by means of an azimuthal plastic-board circle placed below each leaf along the stem of tagged plants (Maddonni *et al.*, 2001). The circle was divided into 16 sectors (22°30' per sector), and sectors 16, 1, 8 and 9 were placed over the line of row direction. For each leaf of tagged plants, the sector number where the projection of the middle part of the midrib occurred was recorded to calculate the frequency of leaves within each sector.

Measurements of photosynthetically active radiation

Photosynthetic photon flux density (PPFD) was measured by using a 1 m long sensor bar (Cavabar, Cavadevices, Argentina) following established procedures (Andrade *et al.*, 1996; Maddonni and Otegui, 1996; Pagano and Maddonni, 2007). To quantify incident photosynthetically active radiation (IPAR), the bar was placed above the canopy. To measure transmitted PAR (TPAR), the bar was immediately positioned below green leaves, but above senesced leaves (approx. 20 cm above the ground). The sensor bar was placed close to the tagged plants diagonally across the rows to fit it between two inter-row spaces. In Exp_1 and Exp_2, three measurements of IPAR and TPAR were recorded per sub-plot close to R_1 at clear mid-days (11.30–13:00 h local time). The fraction of IPAR intercepted by the crop canopy (fIPAR) and the fraction of incident PAR intercepted per plant were calculated according to eqns (2) and (3), respectively.

$$\text{fIPAR} = 1\,(\text{TPAR}/\text{IPAR}) \quad (2)$$

$$\text{fIPARperplant} = \text{fIPAR}/\text{plantdensity} \quad (3)$$

Measurements of R:FR

To describe the light quality environment reaching the base of the plants, measurements of the R:FR were performed at R_1 (only in Exp_2) using a two-channel radiometer (Model SKR 110, Skye Instruments, Powys, UK) with a cosine-corrected head and narrow band filters centred at 660 (R) and 730 nm (FR). The sensor was connected to a hand-held meter for direct instantaneous readout. Four measurements per sub-plot and sensor orientation were performed between 12.00 and 13.00 h local time on a clear day. The sensor was placed close to the base of tagged plants (3–4 cm apart), with its sensing surface perpendicular to the soil and facing towards the four cardinal points. When the sensing surface was pointing to the north and south, records represented light reflected from the inter-row spacing. Conversely, records from the east and west orientations represented light arriving at the base of the plants from the closer plants within the row Table 1.

Photosynthesis and stomatal conductance

An additional field experiment (Exp_3) was carried out during 2015. Plants of each genotype were first cultivated in pots (1.8 L filled with sand, soil and perlite, 3–1–1) in a growth chamber (PPFD, 340 µmol m^{-2} s^{-1}; temperature, 20 °C; photoperiod, 10 h). At V_6, the plants were pricked out to outdoor conditions. Plants were randomly arranged in rows 0.40 m apart at the same low population density used in Exp_1 and Exp_2. Plants were fertilized and irrigated adequately to avoid nutrient deficiencies and water limitations.

At R_1, stomatal conductance (g_s) and net photosynthesis rate (A) were recorded for the ear leaf of five plants per genotype.

TABLE 1. *Values of red:far-red (R:FR) reaching the base of the plants from four cardinal points at R_1 in Exp_2 for WT,* phyB1 *and* phyB2 *lines cultivated at low (9 plants m^{-2}) and high (30 plants m^{-2}) plant densities*

Density	Genotype	North		South		East		West	
		R:FR Mean	s.d.	Mean	s.d.	Mean	s.d	Mean	s.d.
Low	WT	0.50	0.07	0.48	0.08	0.63	0.09	0.57	0.23
	phyB1	0.52	0.05	0.55	0.09	0.66	0.26	0.63	0.24
	phyB2	0.52	0.12	0.54	0.09	0.74	0.15	0.59	0.12
High	WT	0.17	0.04	0.22	0.01	0.24	0.05	0.24	0.09
	phyB1	0.32	0.19	0.31	0.14	0.37	0.08	0.33	0.27
	phyB2	0.19	0.09	0.32	0.01	0.31	0.01	0.28	0.08
	D	0.01		0.003		0.005		0.07	
	G	0.22		0.25		0.58		0.64	
	D × G	0.29		0.94		0.75		0.98	

Each value represents the average of 12 measurements recorded in three sub-plots of each genotype and plant density ($n = 36$).

P-values for plant density (D), genotype (G) effects and their interactions are detailed at the bottom of the table.

Measurements were performed at noon, during a sunny day, using a portable infrared gas analyser system (IRGA) model Li-Cor 6400 (Li-Cor Inc., Lincoln, NE, USA) under saturating light (i.e. 2000 mmol m^{-2} s^{-1} PPFD provided by the 6400-02B LED light source leaf chamber). Air flow and CO_2 concentration in the reference chamber (CO_2R) were automatically controlled by the equipment at 300 mmol s^{-1} and 400 mmol mol^{-1} ppm, respectively. No differences in leaf temperature were recorded between genotypes (30.5 ± 0.5 °C).

Statistical analysis

Traits of Exp_1 and Exp_2 were analysed by using a factorial arrangement, with experiment (Exp_1 and Exp_2) as random effect, and density (low and high) and genotype (WT, *phyB1* and *phyB2*) as fixed effects. The main effects (experiment, plant density and genotype) were analysed by using analysis of variance (ANOVA) followed by Tukey's and LSD Fisher tests to compare pairs of means. In Exp_3, mutant effects on A and g_s were also analysed by using ANOVA followed by Tukey's test.

To evaluate the effect of mutations on the determinants of PGR, we explored the relationships between fIPAR per plant and PLA, and between PGR and fIPAR per plant by linear regressions analysis.

A χ^2 test was used to analyse the spatial orientation of leaves. To evaluate *phyB1* and *phyB2* effects on this trait, leaf azimuthal distribution of each mutant at the low density (i.e. negligible interferences among plants) was compared with that of the WT at the same density. To test the population density effect on the spatial orientation of leaves, the azimuthal leaf distribution of each genotype at the high density (i.e. high interferences among plants) was compared with that at low density. Differences among treatments in azimuthal distribution of leaves were significant ($P < 0.05$) when the estimated χ^2 value was greater than the expected χ^2 with 15 d.f.

RESULTS

Impaired biomass accumulation of the phyB *mutants in the field*

The accumulation of biomass was measured in Exp_1 and Exp_2, and the higher accumulated incident solar radiation during the second field experiment is reflected in its elevated growth, compared with the first experiment. In both cases, the high, compared with the low, population density reduced growth in all three genotypes (Fig. 1). In the WT, from 1000 °Cd after sowing (i.e. beyond the R_1 stage) onwards, biomass per plant was significantly lower at high density than at low density (Fig. 1). At high density, plants of *phyB1* and *phyB2* showed a similar biomass to that of the WT. At low density, both mutants followed the WT pattern up to 1000 °Cd but subsequently grew significantly less than the WT (Fig. 1).

Impaired stem and leaf growth of the phyB *mutants in the field*

The above-ground biomass of vegetative maize plants comprises the stem and the leaves. Therefore, the differences reported in the previous section should be accounted for by effects on the growth of these organs. All genotypes exhibited longer stems at high density than at low plant density (Fig. 2A, B), and this is considered a typical shade-avoidance response. However, contrary to expectation, none of the *phyB* mutants was taller than the WT, and the *phyB1* mutant was actually shorter (Fig. 2A and B, left). This suggests that the shade-avoidance response caused by the lack of phyB1 was overcompensated by its compromised growth capacity (see Fig. 1).

At low plant density, the stems of *phyB1* and *phyB2* were thinner than those of the WT plants, and high plant density reduced stem diameter of the WT, eliminating the difference from the mutants (Fig. 2C, D; Table 2).

The PLA was not significantly affected by plant density but, at both densities, it was reduced in the *phyB1* and *phyB2* mutants compared with the WT (Fig. 3A). Both mutants had smaller leaves than the WT, and plants of *phyB1* also had fewer leaves than the WT (Table 2). At most, modest effects of the mutations or population density on cell number per unit area were observed (Supplementary Data Figs S2 and S3; Table S2). Since the mutations had no effect on cell area, their impact on leaf area is considered to be mainly the result of a reduced number of cells.

In the WT, the thickness of the ear leaf decreased with plant density (Figs 3B and 4A, D). However, in the *phyB1* and *phyB2* mutants, leaf thickness was constitutively reduced, i.e. thinner

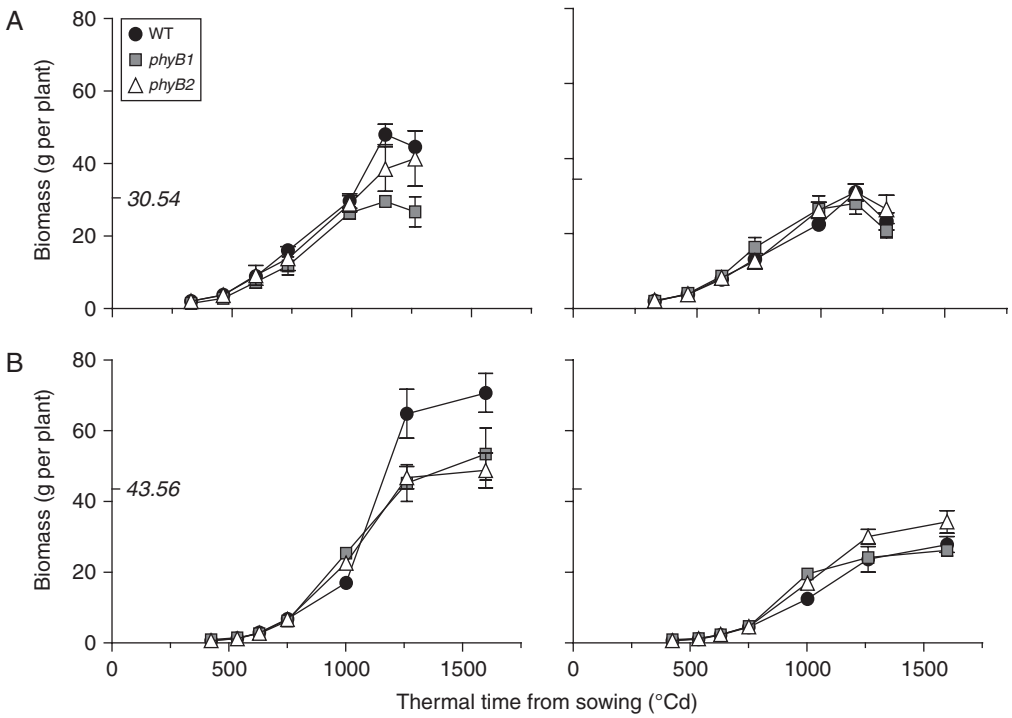

FIG. 1. The *phyB1* and *phyB2* mutations impair biomass accumulation in field-grown maize plants. Plant biomass as a function of thermal time from sowing for the WT, *phyB1* and *phyB2* cultivated at low (left side graphs) and high (right side graphs) plant density in Exp_1 (A) and Exp_2 (B). Data are means (n = 30) ± s.e. Marks on the y-axis indicate average plant biomass in each experiment for all genotypes and plant densities.

than that of the WT at low density and similar to that of the WT at high density (Figs 3B and 4B, E, C, F).

In summary, the reduced biomass of the *phyB1* and *phyB2* mutants implies reduced stem width (and in *phyB1* stem height) and reduced leaf area and thickness.

Deficient light capture in the phyB *mutants*

At low density, differences in plant biomass between the WT and the *phyB1* and *phyB2* mutants could be the result of effects on the ability to capture light per plant and/or the capacity to produce biomass per unit of intercepted light. In order to explore if the mentioned changes of PLA affected the capacity of plants for light capture, fIPAR per plant values of each treatment combination were plotted against the corresponding PLA. At low density, a positive linear function adequately described the response of fIPAR per plant to PLA without any obvious genotype or experiment bias (Fig. 5A). Hence, reduced PLA determined by mutations of *phyB* compromised fIPAR per plant. At high population density, changes in PLA caused by the mutations were not reflected in variations in fIPAR per plant because under this crowded condition increased PLA enhanced mutual shading among leaves (Fig. 5B), reducing the amount of light intercepted per leaf.

Azimuthal leaf distribution did not differ among genotypes or between population densities (Supplementary Data Fig. S3). Although horizontal leaf distribution responds to the gradients of R:FR (Maddonni *et al.*, 2002) and these are typically perceived by phyB, the lack of response is not surprising here because the leaves were pre-oriented towards the inter-row space by the position of seeds at sowing. Therefore, changes in fIPAR per plant caused by the *phyB1* or *phyB2* mutations were largely the result of their effects on PLA, and not of differential horizontal reorientation of the leaves.

Relationship between light interception and growth

Since PGR around R_1 is important for grain yield in maize (Andrade *et al.*, 1999), we conducted a more detailed analysis focused on this particular phenological stage. Both *phyB1* and *phyB2* showed reduced PGR around R_1 (Table 2). A positive linear regression adequately described the relationship between PGR and fIPAR per plant for the whole data set (Fig. 6A). No biases among genotypes or population densities were observed for this trend. This indicates that the effects of *phyB1* and *phyB2* on PGR were largely the result of their reduction in leaf expansion and not of impaired PGR per fIPAR per plant. In support of this conclusion, no effects of the *phyB* mutations on maximum photosynthesis, stomatal conductance or stomatal density were observed (Supplementary Data Fig. S4; Table S1).

Grain yield per plant

Plant grain yield was linearly related to PGR around R_1 (Fig. 6B). At the lowest plant density, most plants had a single ear (fertility index slightly below 1), with some reduction caused by the *phyB1* mutation (Table 2). At the highest density, the

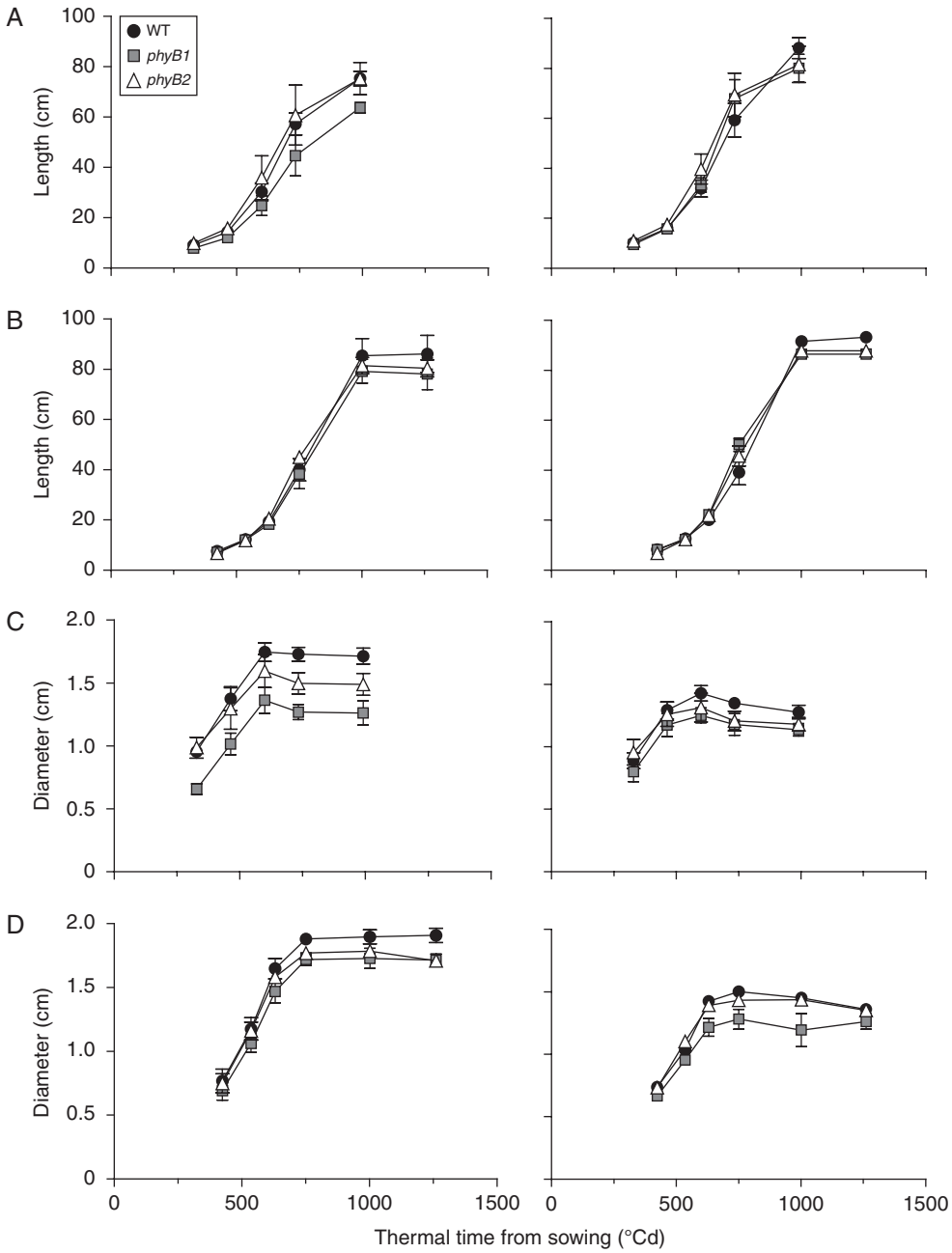

FIG. 2. The *phyB1* and *phyB2* mutations affect stem growth in field-grown maize plants. Stem length (A and B) and stem diameter (C and D) as a function of thermal time from sowing for the WT, *phyB1* and *phyB2* cultivated at low (left side graphs) and high (right side graphs) plant density in Exp_1 (A and C) and Exp_2 (B and D). Data are means (n = 30) ± s.e.

latter proportion fell to approximatley one ear for every two plants, except for the *phyB2* mutant, which retained a high fertility index (Table 2).

DISCUSSION

A critical function of phyB is to perceive the differences between the high R:FR typical of sunlight in unshaded places and the low R:FR typical of crowded vegetation environments (Casal, 2013*a*, *b*; Ballaré and Pierik, 2017). The results presented here indicate that the *phyB1* and *phyB2* mutations are able to compromise growth of maize plants cultivated at relatively low densities under full sunlight in the summer season. This implies that the inability to perceive the light cues that indicate a high availability of resources (e.g. high radiation for photosynthesis in open places) sets a lower growth capacity for maize plants, which become unable to take full advantage of these extra resources.

A mutation at the genes encoding either the phyB1 or the phyB2 photoreceptors was enough to reduce leaf area per plant (Fig. 3). This effect was largely caused by the presence of smaller leaves. As the area of each cell was unaffected, impaired leaf expansion was largely due to a reduced number of

TABLE 2. *Plant height, stem diameter, mean leaf size, total leaf number, plant growth rate (PGR) around silking, and fertility index and plant grain yield of the maize plants of the WT,* phyB1 *and* phyB2 *cultivated at low (9 plants m^{-2}) and high (30 plants m^{-2}) plant densities in two experiments*

		Plant height (cm)		Stem diameter (cm)		Mean leaf size (cm^2)		Total leaf number		PGR (g per plant d^{-1})	Fertility index	Grain yield (g per plant)		
Density	Genotype	Mean	s.d.	Mean	s.d.	Mean	s.d.	Mean	s.d.	Mean	Mean	s.d.	Mean	s.d.
Low	WT	80	10	1.81	0.14	205	24	13	0.44	1.78	0.95	0.08	27	10
	phyB1	70	10	1.49	0.27	170	38	12	0.29	0.95	0.78	0.15	14	9
	phyB2	77	8	1.60	0.16	151	21	13	0.50	1.18	0.97	0.05	23	8
High	WT	90	5	1.32	0.08	185	15	13	0.15	0.70	0.55	0.12	8	2
	phyB1	83	6	1.20	0.11	144	25	12	0.39	0.46	0.48	0.29	4	1
	phyB2	84	8	1.27	0.11	151	27	13	0.64	0.68	0.82	0.17	12	6
	Exp	0.035		0.001		0.087		0.030		0.653	0.045		0.091	
	D	0.116		0.003		0.336		0.725		0.001	0.011		0.002	
	G	0.005		0.000		0.000		0.000		0.000	0.000		0.000	
	Exp × D	0.688		0.256		0.544		0.964		0.037	0.410		0.101	
	Exp × G	0.585		0.074		0.210		0.500		0.109	0.016		0.081	
	D × G	0.497		0.012		0.253		0.603		0.002	0.031		0.002	
	Exp × D × G	0.574		0.093		0.116		0.688		0.394	0.359		0.163	

Mean values and the s.d. of the means are presented (n = 360).

P-values for Exp, plant density (D) and genotype (G) effects and their interactions are detailed.

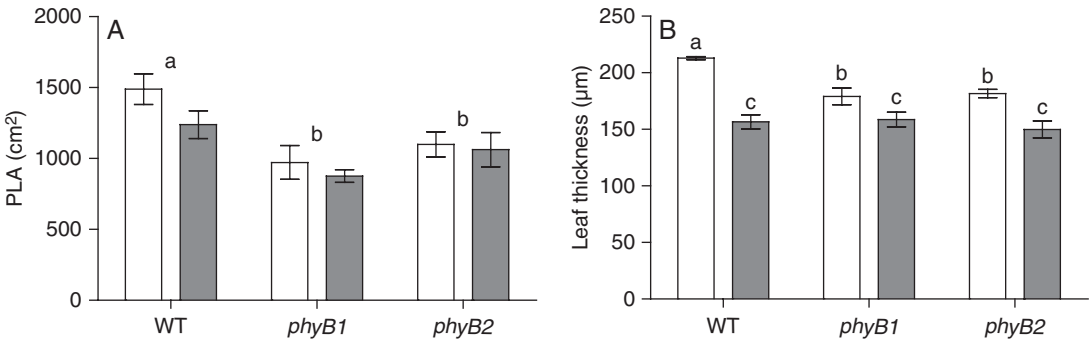

FIG. 3. The *phyB1* and *phyB2* mutations reduce leaf growth in field-grown maize plants. (A) Plant leaf area (PLA) for the WT, *phyB1* and *phyB2* cultivated at low (9 plants m^{-2}, white columns) and high (30 plants m^{-2}, grey columns) plant density. Each column indicates the average of each genotype combining Exp_1 and Exp_2 (n = 60). Lower case letters indicate significant differences ($P < 0.05$) among genotypes independently of plant density. (B) Leaf thickness values (mean and s.e.) of each genotype at low (9 plants m^{-2}, white columns) and high (30 plants m^{-2}, grey columns) plant density. Different letters above bars indicate significant differences ($P < 0.05$) among genotype × plant density interactions.

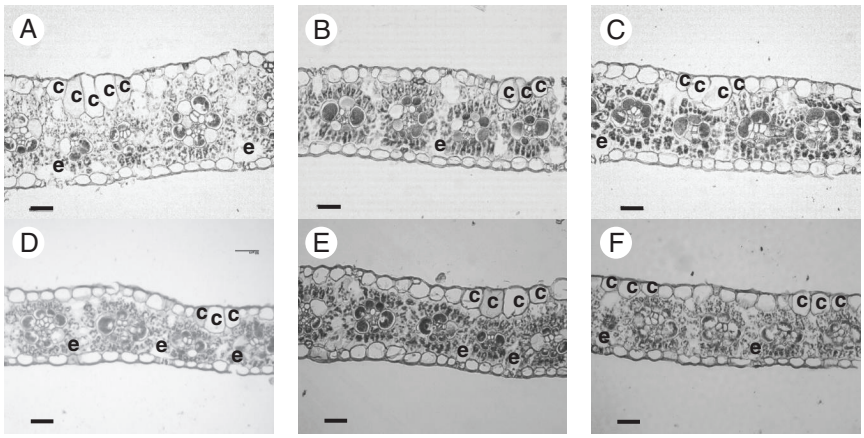

FIG. 4. The *phyB1* and *phyB2* mutations reduce leaf thickness in field-grown maize plants. Photographs of transversal sections of the leaf subtending the apical ear for the WT (A and D), *phyB1* (B and E) and *phyB2* (C and F) cultivated at low (A, B, C) and high (D, E, F) plant density in Exp_2 (n = 27). e, stomata; c, bulliform cells. Scale bars = 50 µm.

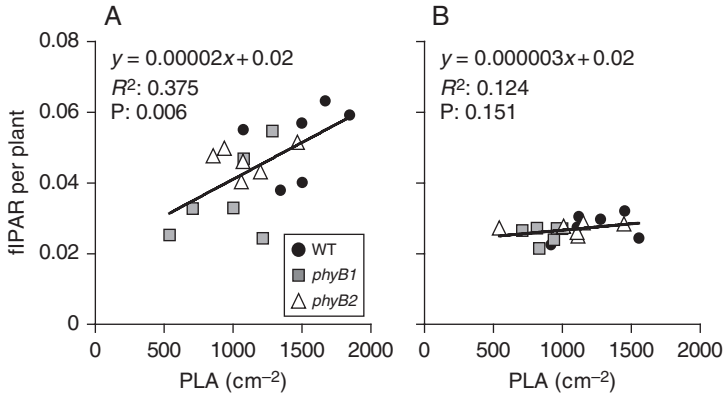

FIG. 5. The impact of plant leaf area on light interception at different population densities. Fraction of incident photosynthetically active radiation (fIPAR) intercepted per plant for the WT, *phyB1* and *phyB2* as a function of PLA at low (A) and high (B) plant density ($n = 36$). *P*: significance of the slope.

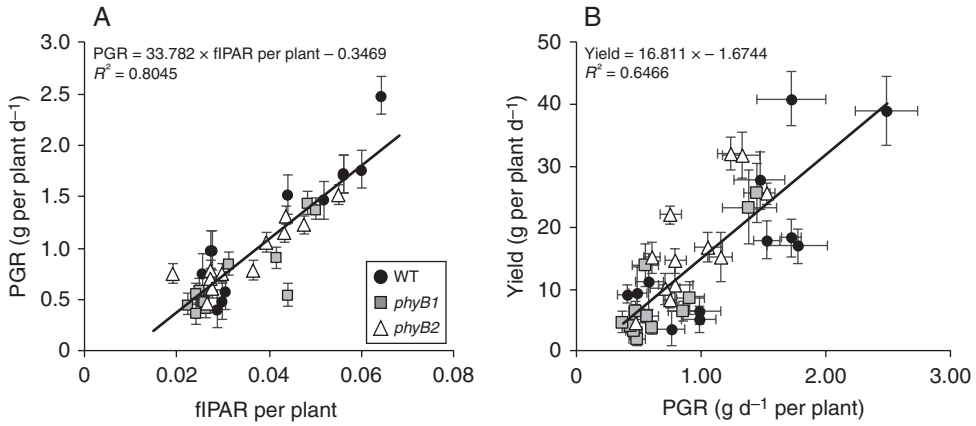

FIG. 6. The relationship between light interception and growth and between growth and grain yield. (A) Plant growth rate (PGR) as a function of the fraction of incident photosynthetically active radiation intercepted (fIPAR) per plant and (B) yield per plant as function of PGR for the WT, *phyB1* and *phyB2*. Each point represents the mean PGR, fIPAR per plant and yield per plant of ten plants per plot in both experiments ($n = 18$). Bars represent the s.e.m.

cells (Supplementary Data Figs S2 and S3; Table S2). In turn, the effects on leaf area compromised the ability of the *phyB1* and *phyB2* mutants to capture fully the extra light for photosynthesis available under lower population densities (Fig. 5). Finally, the impaired light capture caused reduced growth (Fig. 6), which is consistent with previous observations indicating that maize crop growth at this stage is limited by light capture (Tetio-Kagho and Gardner, 1988; Maddonni and Otegui 1996; Maddonni *et al.*, 2001).

As expected (Andrade *et al.*, 1999), differences in PGRs around female flowering (i.e. the critical period for kernel setting in maize) caused by population density and the presence of the *phyB1* mutation translated into differences in plant grain yield (Fig. 6B). However, despite the different PGRs between the WT and *phyB2* at low density, plant grain yield of *phyB2* did not differ from that of the WT because of the high fertility index of *phyB2*, which was retained even at the high density, a condition that negatively affects this trait (Echarte and Andrade, 2003). Confirmation of this phenotype and the observed differences in leaf number (Table 2) would require an independent *phyB2* allele, not available at present. Conversely all the other phenotypes reported here are genuine because they are observed in both the *phyB1* and *phyB2* mutants.

The *phyB* mutations can also decrease overall growth, biomass accumulation, total protein levels and cellulose synthase expression in *A. thaliana* grown under controlled conditions (Yang *et al.*, 2016). It has been proposed that phy would be a major environmental driver of plant biomass production and regulate the transition between growth-intensive and stress-resilient states (Yang *et al.*, 2016). However, while in *A. thaliana phyB* mutations reduced the stomatal index, stomatal conductance and photosynthesis rate (Boccalandro *et al.*, 2009; Liu *et al.*, 2012), maximum photosynthesis and stomatal density (Supplementary Data Figs S1, S2 and S4; Table S2) were not affected by the *phyB1* or *phyB2* mutations in maize. The effects of low R:FR and *phyB* mutations on leaf expansion depend on the species and growth conditions (Casal, 2012).

When crops are grown at increasing population densities, there is a reduction in the amount of resources (e.g. light for photosynthesis) available per plant, due to sharing among a larger numbert of individuals. In addition, plants experience a reduction of phyB activity caused by the low R:FR (Casal, 2013*a*, *b*; Ballaré and Pierik, 2017). In the *phyB1* and *phyB2* mutants, the activity of phyB is reduced genetically even under the higher R:FR of open places. Therefore, if the response of a given trait to plant density is mediated at least partially by the

reduction in R:FR under crowed conditions, the phyB mutations would be expected to affect that trait in the same direction. This is the case for the reduction of leaf thickness caused by increasing plant density, which was completely absent in the *phyB1* and *phyB2* mutants (Figs 3B an 4A, D), indicating that this density response in the WT would be largely mediated by the perception of a low R:FR by phyB. High plant density and the *phyB1* and *phyB2* mutations also reduced stem diameter, but the mutants retained at least partial response to density (Fig. 2). This suggests that the inactivation of phyB1 or phyB2 by low R:FR would reduce stem diameter but there would be some degree of redundancy among photoreceptors (Mazzella *et al.*, 2001; Strasser *et al.*, 2010) because mutating one of them does not fully eliminate the response. Although the increase in stem stature in response to the reduction of phyB activity caused by mutual plant shading is arguably the most typical shade-avoidance response and the stem was actually tall in the highest density, the *phyB1* and *phyB2* mutants were not taller than the WT. This suggests that the shade-avoidance response was probably compromised in these mutants by their reduced growth capacity. Maize crops typically reduce PLA in response to increasing densities (Pommel and Bonhomme, 1998; Maddonni *et al.*, 2001). The reduced PLA of the *phyB1* and *phyB2* mutants suggests that this plant density effect could also be at least partially mediated by the perception of low R:FR by phyB.

Here we show that the loss-of-function *phyB1* or *phyB2* mutations reduce the capacity of maize plants to grow in response to the additional resources that become available when the plant population is reduced. Furthermore, we show that stem thickness, which is an important variable in the definition of the risk of lodging, is also controlled by phyB. These observations place the signals perceived by phyB within the factors of significance to determine the performance of agricultural crops in addition to the resources provided by the environment. Under natural radiation, the activity of phyB depends on the balance of light and thermal reactions (Sellaro *et al.*, 2018), giving ample room for variations dependent on the magnitude of these reactions in different genetic backgrounds. Actually, natural genetic variability at the *PHYB* locus affects sensitivity to light cues in *A. thaliana* (Filiault *et al.*, 2008). Therefore, it would be interesting to evaluate whether natural genetic variability at the *PHYB* locus affects the performance of maize plants in the field.

SUPPLEMENTARY DATA

Supplementary data are available online at https://academic.oup.com/aob and consist of the following. Figure S1: leaf abaxial epidermis. Figure S2: leaf adaxial epidermis. Figure S3: leaf horizontal position. Figure S4: net photosynthesis and stomatal conductance. Table S1: allometric models to estimate plant biomass. Table S2: cell and stomata density in leaves.

ACKNOWLEDGEMENTS

We thank the Maize Genetics Corporation Stock Center for providing seeds used in this work, Juan Fuentes and Luis Hercun for their assistance in the field experiments, Edmundo Ploschuk for his support with photosynthesis measurements, and Benjamín Aguilar Ortega for his comments on the text. This work was supported by the University of Buenos Aires (UBACyT G20020100100551) and PICT 2012-1260. G.W. received a post-graduate scholarship from the University of Buenos Aires. G.A.M. and J.C. are members of the National Research Council of Argentina (CONICET).

LITERATURE CITED

Andrade FH, Otegui ME, Vega C. 1996. Intercepted radiation at flowering and kernel number in maize. *Agronomy Journal* **92**: 92–97.

Andrade FH, Vega C, Uhart S, Cirilo A, Cantarero M, Valentinuz O. 1999. Kernel number determination in maize. *Crop Science* **39**: 453–459.

Ballaré CL, Pierik R. 2017. The shade-avoidance syndrome: multiple signals and ecological consequences. *Plant, Cell & Environment* **40**: 2530–2543.

Boccalandro HE, Rugnone ML, Moreno JE, *et al.* 2009. Phytochrome B enhances photosynthesis at the expense of water-use efficiency in Arabidopsis. *Plant Physiology* **150**: 1083–1092.

Borrás L, Maddonni G, Otegui M. 2003. Leaf senescence in maize hybrids: plant population, row spacing and kernel set effects. *Field Crops Research* **82**: 13–26.

Casal JJ. 2012. Shade avoidance. *The Arabidopsis Book* **10**: 1–19.

Casal JJ. 2013*a*. Canopy light signals and crop yield in sickness and in health. *ISRN Agronomy* **2013**: 1–16.

Casal JJ. 2013*b*. Photoreceptor signaling networks in plant responses to shade. *Annual Review of Plant Biology* **64**: 403–27.

Dizeo de Strittmatter CG. 1973. Nueva técnica de diafanización. *Boletín de la Sociedad Argentina de Botánica* **15**: 126–129.

Echarte L, Andrade F. 2003. Harvest index stability of Argentinean maize hybrids released between 1965 and 1993. *Field Crops Research* **82**: 1–12.

Echarte L, Tollenaar M. 2006. Kernel set in maize hybrids and their inbred lines exposed to stress. *Crop Science* **46**: 870–878.

Filiault DL, Wessinger CA, Dinneny JR, *et al.* 2008. Amino acid polymorphisms in Arabidopsis phytochrome B cause differential responses to light. *Proceedings of the National Academy of Sciences, USA* **105**: 3157–3162.

Johansen DA. 1940. *Plant microtechnique*. New York: McGraw-Hill.

Kulshreshtha R, Kumar N, Balyan HS, *et al.* 2005. Structural characterization, expression analysis and evolution of the red/far red sensing photoreceptor gene, phytochrome C (PHYC), localized on the 'B' genome of hexaploid wheat (*Triticum aestivum* L.). *Planta* **221**: 675–689.

Laserna MP, Maddonni GA, López CG. 2012. Phenotypic variations between non-transgenic and transgenic maize hybrids. *Field Crops Research* **134**: 175–184.

Liu J, Zhang F, Zhou J, Chen F, Wang B, Xie X. 2012. Phytochrome B control of total leaf area and stomatal density affects drought tolerance in rice. *Plant Molecular Biology* **78**: 289–300.

Maddonni GA, Otegui ME. 1996. Leaf area, light interception, and crop development in maize. *Field Crops Research* **48**: 81–87.

Maddonni GA, Otegui ME. 2004. Intra-specific competition in maize: early establishment of hierarchies among plants affects final kernel set. *Field Crops Research* **85**: 1–13.

Maddonni GA, Otegui ME, Cirilo AG. 2001. Plant population density, row spacing and hybrid effects on maize canopy architecture and light attenuation. *Field Crops Research* **71**: 183–193.

Maddonni GA, Otegui E, Andrieu B, Chelle M, Casal JJ. 2002. Maize leaves turn away from neighbors. *Plant Physiology* **130**: 1181–1189.

Mathews S, Sharrock RA. 1997. Phytochrome gene diversity. *Plant, Cell & Environment* **20**: 666–671.

Mazzella MA, Cerdán PD, Staneloni RJ, Casal JJ. 2001. Hierarchical coupling of phytochromes and cryptochromes reconciles stability and light modulation of Arabidopsis development. *Development* **128**: 2291–2299.

Montgomery EC. 1911. *Correlation studies in corn. 24th Annual Report*. Nebraska: Agricultural Experiment Station.

Pagano E, Maddonni GA. 2007. Intra-specific competition in maize: early established hierarchies differ in plant growth and biomass partitioning to the ear around silking. *Field Crops Research* **101**: 306–320.

Page ER, Tollenaar M, Lee EA, Lukens L, Swanton CJ. 2009. Does the shade avoidance response contribute to the critical period for weed control in maize (*Zea m*ays)? *Weed Research* **49**: 563–571.

Page ER, Liu W, Cerrudo D, Lee EA, Swanton CJ. 2011. Shade avoidance influences stress tolerance in maize. *WeedScience* **59**: 326–334.

Pommel B, Bonhomme R. 1998. Variations in the vegetative and reproductive systems in individual plants of an heterogeneous maize crop. *European Journal of Agronomy* **8**: 39–49.

Ritchie SW, Hanway JJ, Benson GO. 1993. *How a corn plant develops*. Special Report No. 48, Iowa State University of Science and Technology Cooperative Extension Service, Ames, Iowa.

Sangoi L, Gracietti M, Rampazzo C, Bianchetti P. 2002. Response of Brazilian maize hybrids from different eras to changes in plant density. *Field Crops Research* **79**: 39–51.

Sattin M, Zuin MC, Sartorato I. 1994. Light quality beneath field-grown maize, soybean and weat canopies – red:far red variations. *Physiologia Plantarum* **91**: 322–328.

Sellaro R, Smith RW, Legris M, Fleck C, Casal JJ. 2018. Phytochrome B dynamics departs from photoequilibrium in the field. *Plant, Cell & Environment* (in press).

Sheehan MJ, Farmer PR, Brutnell TP. 2004. Structure and expression of maize phytochrome family homeologs. *Genetics* **167**: 1395–405.

Sheehan MJ, Kennedy LM, Costich DE, Brutnell TP. 2007. Subfunctionalization of PhyB1 and PhyB2 in the control of seedling and mature plant traits in maize. *The Plant Journal* **49**: 338–53.

Smith H, Casal JJ, Jackson GM. 1990. Reflection signals and the perception by phytochrome of the proximity of neighbouring vegetation. *Plant, Cell & Environment* **13**: 73–78.

Stewart DW, Dwyer LM. 1999. Mathematical characterization of leaf shape and area of maize hybrids. *Crop Science* **39**: 422–427.

Strasser B, Sánchez-Lamas M, Yanovsky MJ, Casal JJ, Cerdán PD. 2010. *Arabidopsis thaliana* life without phytochromes. *Proceedings of the National Academy of Sciences, USA* **107**: 4776–81.

Tetio-Kagho F, Gardner FP. 1988. Responses of maize to plant population density. I. Canopy development, light relationships, and vegetative growth. *Agronomy Journal* **80**: 930–935.

Toler JE, Murdock EC, Stapleton GS, Wallace SU. 1999. Corn leaf orientation effects on light interception, intraspecific competition, and grain yields. *Journal of Production Agriculture* **12**: 396–399.

Tollenaar M, Dwyer LM, Stewart DW. 1992. Ear and kernel formation in maize hybrids representing three decades of grain yield improvement in Ontario. *Crop Science* **32**: 432–438.

Yang D, Seaton DD, Krahmer J, Halliday KJ. 2016. Photoreceptor effects on plant biomass, resource allocation, and metabolic state. *Proceedings of the National Academy of Sciences, USA* **113**: 7667–7672.